ANTIMICROBIAL AGENTS AND CHEMOTHERAPY, Aug. 2010, p. 3079–3085 Vol. 54, No. 8
0066-4804/10/$12.00 doi:10.1128/AAC.00122-10

Cell Wall Thickening Is Not a Universal Accompaniment of the Daptomycin Nonsusceptibility Phenotype in *Staphylococcus aureus*: Evidence for Multiple Resistance Mechanisms▽

Soo-Jin Yang,[1]* Cynthia C. Nast,[2,3] Nagendra N. Mishra,[1] Michael R. Yeaman,[1,3] Paul D. Fey,[4] and Arnold S. Bayer[1,3]

Los Angeles Biomedical Research Institute, Torrance, California[1]; Cedar-Sinai Medical Center, Los Angeles, California[2]; David Geffen School of Medicine at UCLA, Los Angeles, California[3]; and University of Nebraska Medical Center, Omaha, Nebraska[4]

Received 27 January 2010/Returned for modification 30 April 2010/Accepted 17 May 2010

The mechanism(s) of daptomycin (DAP) resistance (DAP^r) is incompletely defined. Thickened cell walls (CWs) acting as either a mechanical barrier or an affinity trap for DAP have been purported to be a major contributor to the DAP^r phenotype. To this end, we studied an isogenic set of methicillin-resistant *Staphylococcus aureus* (MRSA) isolates (pulsotype USA 300) from the bloodstream of a DAP-treated patient with endocarditis in which serial strains exhibited increasing DAP^r. Of interest, the DAP^r isolate differed from its parental strain in several parameters, including acquisition of a point mutation within the putative synthase domain of the *mprF* gene in association with enhanced *mprF* expression, increased synthesis of lysyl-phosphotidylglycerol, an enhanced positive envelope charge, and reduced DAP surface binding. Transmission electron microscopy (TEM) revealed no significant increases in CW thickness in the two DAP^r isolates (MRSA 11/21 and REF2145) compared with that in the DAP-susceptible (DAP^s) parental strain, MRSA 11/11. The rates of Triton X-100-induced autolysis were also identical for the strain set. Furthermore, among six additional clinically isolated DAP^s/DAP^r *S. aureus* strain pairs, only three DAP^r isolates exhibited CWs significantly thicker than those of the respective DAP^s parent. These data confirm that CW thickening is neither universal to DAP^r *S. aureus* nor sufficient to yield the DAP^r phenotype among *S. aureus* strains.

Daptomycin (DAP) is a cyclic lipopeptide antibiotic active against a wide range of Gram-positive organisms, including methicillin-resistant *Staphylococcus aureus* (MRSA) strains, vancomycin (VAN)-intermediate *S. aureus* (VISA), and vancomycin-resistant *S. aureus* (VRSA) (23, 24, 28, 32). However, increasing numbers of reports have described development of *in vitro* DAP resistance (DAP^r) in association with DAP clinical treatment failures in a variety of *S. aureus* infections (2, 9, 12, 26).

The exact mechanism(s) of DAP^r remains unknown. However, through previous studies in our laboratory (11, 16, 36, 37), we have found that the pathways which are associated with DAP^r appear to be multifactorial and may differ among DAP^r *S. aureus* strains. Recently, using isogenic sets of *S. aureus* clinical isolates from a DAP-treated patient with recalcitrant endocarditis, we found a variety of cell membrane (CM) and cell envelope alterations associated with the DAP^r phenotype (11), including those involving membrane fluidity, membrane phospholipid (PL) composition and asymmetry, surface charge, relative *in vitro* cross-resistance to certain CM-targeting cationic host defense antimicrobial peptides (CAPs), and DAP binding (11, 36).

In addition to these membrane phenotypic changes, alterations in cell wall (CW) structure and/or function have been proposed to be involved in DAP^r. For example, Julian et al. described the reduction of peptidoglycan cross-linking and a reduced degree of muramic acid O-acetylation in DAP^r VISA strains (12). Cui et al. (6) also described a positive correlation between DAP^r and vancomycin resistance in VISA strains. In both studies, a notable increase in CW thickness was observed, suggesting a potential role for a CW-based physical barrier to DAP reaching its ultimate cell membrane target. We have also observed thickened CWs in one *in vitro* passage-derived DAP^r *S. aureus* strain (16). However, it is not clear whether such increased CW thickness is a universal phenotype among DAP^r *S. aureus* strains, especially among clinical isolates.

In the present study, we further investigated the putative correlation between CW thickness and DAP^r by examining several additional isogenic DAP-susceptible (DAP^s) and DAP^r sets of *S. aureus* bloodstream isolates from DAP-treated patients.

(Although the currently accepted term for reduced *in vitro* susceptibility to daptomycin is "nonsusceptible," we use the term "daptomycin-resistant" [DAP^r] in this paper for a more facile presentation.)

MATERIALS AND METHODS

Bacterial strains and growth conditions. The primary strain set used in this study was isolated from a patient with recalcitrant endocarditis. The clinical details related to this patient and to the pulsed-field gel electrophoresis (PFGE)-identical, isogenic strain set (strains MRSA 11/11, MRSA 11/17, MRSA 11/21, REF2145) have been described previously (19). This strain set was pulsotype USA 300 (MLST type 8). Strain MRSA 11/11 was the initial bloodstream isolate recovered prior to VAN or DAP therapy and was DAP^s. The second strain (MRSA 11/17) was isolated after 5 days of VAN therapy. The last two isolates

* Corresponding author. Mailing address: LA Biomedical Research Institute at Harbor-UCLA, 1124 West Carson Street, RB-2, Rm. 230, Torrance, CA 90502. Phone: (310) 222-6423. Fax: (310) 782-2016. E-mail: sjyang@labiomed.org.

▽ Published ahead of print on 24 May 2010.

TABLE 1. Cell wall thickness measurements of four recently isolated DAP^s and DAP^r clinical strain sets studied in addition to the primary strain set

Strain pair[a]	MIC (μg/ml)		CW thickness (nm)	Reference or source
	DAP	VAN		
CB1482	0.5	2	38.62 ± 4.28	8
CB184	4	2	40.02 ± 4.66	8
CB5053	0.5	1	33.44 ± 3.42	This study
CB5054	2	2	35.22 ± 3.76	This study
CB5035	0.38	2	38.03 ± 4.15	This study
CB5036	2	2	32.66 ± 3.27	This study
BMC1001	0.5	2	32.28 ± 3.91	This study
BMC1002	2	4	52.40 ± 7.04[b]	This study

[a] All clinical strain pairs were isolated from the bloodstream.
[b] $P < 0.01$ versus the parental strain.

(MRSA 11/21 and REF2145) were subsequently obtained on days 4 and 7 of DAP therapy, respectively, and found to be DAP^r. The DAP MICs for strains MRSA 11/11, MRSA 11/17, MRSA 11/21, and REF2145 in this strain set, determined by standard Etest, were 1, 1, 3, and 4 μg/ml, respectively (19). Of interest, the DAP^r strains were found to have a single nucleotide polymorphism within the *mprF* gene at position 345 (Thr to Ala), which maps to the putative synthase domain of this gene (7, 19). The oxacillin MIC for the initial isolate (isolate 11/11), determined by standard Etest, was 32 μg/ml, while for the last isolate (REF2145), the MIC was 6 μg/ml, demonstrating a "seesaw" effect, as described previously (16). The VAN MICs determined by Etest were 2 μg/ml for all strains in this strain set. The strains in the strain set were also susceptible to the following agents: linezolid, quinupristin-dalfopristin, trimethoprim-sulfamethoxazole, and gentamicin (19).

All strains were grown in either tryptic soy broth (TSB; Difco Laboratories, Detroit, MI) or Mueller-Hinton (MH) broth (Difco Laboratories). Liquid cultures were grown in Erlenmeyer flasks at 37°C with shaking (250 rpm) in a volume that was no greater than 10% of the flask volume. DAP was purchased from Cubist Pharmaceuticals (Lexington, MA) and reconstituted according to the manufacturer's recommendations. All DAP assays were done in the presence of 50 μg/ml calcium, as recommended by the manufacturer.

The primary strain set described above was analyzed for a number of parameters, including cell membrane and cell envelope phenotypes, transcription of two genes involved in maintenance of the cell surface positive charge (*mprF* and *dltA*), and CW thickness, determined by transmission electron microscopy (TEM) (see details below). We also studied six additional DAP^s/DAP^r clinical strain pairs for comparison of their CW thicknesses by TEM (Table 1). Two of these strain pairs have been described previously and were used to provide an overall comparison with the primary strain set in terms of the cell membrane and cell envelope parameters described above, in addition to CW thickness (11, 36, 37). Four other strain sets (courtesy of Aileen Rubio) were selected from the Cubist Pharmaceutical's Registry of DAP^s/DAP^r strain pairs by an individual not involved in our data analyses and were used exclusively for CW thickness comparisons. The selection of the strains was based on the following prioritization: (i) recent clinical strains (bloodstream isolates) and (ii) strains found to be isogenic by PFGE. Their DAP and VAN MICs were determined by standard Etest and are listed in Table 1. We also included a previously described DAP^s/DAP^r strain set selected by *in vitro* passage in DAP as a comparator (8, 16).

Population analyses. Population analyses of MRSA 11/11 and REF2145 upon exposure to a range of DAP and VAN concentrations were performed as described before (17). Briefly, after the strains were grown overnight in TSB (~5×10^9 CFU/ml), serial 10-fold dilutions of the cultures were plated onto MH agar containing DAP or VAN at various concentrations. For DAP and VAN, the range of concentrations tested was 0.0625 to 32 μg/ml, to encompass sublethal to lethal drug levels. The lower limit of detection in these assays was set at 2 $\log_{10}$ CFU/ml. To provide a quantification of this assay, the area under the concentration-time curve (AUC) of the population analysis curves for each strain was determined using the trapezoidal rule (Microcal Origin software, version 5.0; Microcal Software Inc., Northampton, MA) (13).

CAP susceptibility testing. Recent studies showed a temporal correlation between *in vivo* development of DAP^r and relative *in vitro* cross-resistance to several mammalian host defense CAPs, including the α-defensin human neutrophil peptide 1 (hNP-1) from polymorphonuclear leukocytes and thrombin-induced platelet microbicidal proteins (tPMPs) from mammalian platelets (11, 36). hNP-1 was purchased from Peptide International (Louisville, KY), and tPMP-1 preparations were obtained as described previously (38, 40). In addition, RP-1 (a synthetic CAP modeled in part upon the microbicidal domain of tPMP-1 and with a mode of action identical to that of the native peptide) (33, 39) was substituted for tPMP-1 in several of the assays requiring higher concentrations of peptide. *In vitro* bactericidal assays were performed with the tPMP-1 preparation (bioactivity, 1 μg/ml), hNP-1 (20 μg/ml), and RP-1 (3 μg/ml), as described before, using a 2-h CAP exposure time in a microdilution method (11, 34). Data were expressed as the percentage of surviving CFU (±standard deviation [SD]) of CAP-exposed cells compared to the numbers of unexposed control cells over the 2-h exposure period. At least two independent experiments were performed with each peptide.

Peptide binding assays. To determine the relationship between the peptide association with *S. aureus* cells and DAP^r in the primary strain set, RP-1 (40 μg/ml), DAP (6 μg/ml), or VAN (8 μg/ml) was added to 10^8 CFU of each *S. aureus* strain; and the mixture was incubated for 10 min and centrifuged to pellet the cells. The supernatants were then analyzed for residual unbound peptides by a radial diffusion assay, using *Bacillus subtilis* ATCC 6633 as the indicator strain, as described before (11, 38); the amount of unbound peptide was calculated by comparing the resulting zone sizes with the respective peptide concentration-zone size standard curves. At least two independent assays were performed on separate days.

Comparison of relative net cell surface charge. Our prior investigations of DAP^r *S. aureus* strains indicated a frequent alteration of the net cell surface charge compared to that of the respective DAP^s parental strains (11, 16, 36). For these assays, we compared the relative net cell surface charge of *S. aureus* strains by quantifying the association of the highly cationic molecule cytochrome *c* (pI 10; Sigma) to the staphylococcal surface (15, 21). The amount of cytochrome *c* remaining in the postcentrifugation supernatant after a 10-min binding interaction with *S. aureus* cells was quantified spectrophotometrically at an optical density at 530 nm (OD_{530}). The more unbound cytochrome *c* that was detected in the supernatant, the more that a positive charge existed on the bacterial cell surface. The data shown are the means (±SDs) of the amount of unbound cytochrome *c* from three independent experiments.

Membrane phospholipid profiles. Previous studies from our laboratory have shown a correlation between altered membrane PL profiles and DAP^r. These observations particularly focused upon the proportion of the positively charged PL species lysyl-phosphotidylglycerol (LPG) which was synthesized and/or translocated to the outer cystoplasmic membrane leaflet, i.e., phenotypes encoded by *mprF* (7, 11, 37). Membrane PLs were extracted from each of the *S. aureus* isolates in the primary strain set by standard methods (1, 18). The three major PLs (phosphotidylglycerol [PG], LPG, and cardiolipins [CLs]) were separated by two-dimensional thin-layer chromatography (TLC), collected from the plates, and then quantified spectrophotometrically, as described before (11, 18). The proportion of synthesized LPG which was translocated to the outer cell membrane leaflet was quantified spectrophotometrically, as detailed before, using the LPG outer membrane-specific probe fluorescamine (16, 18). The detailed methodologies for detecting and quantifying total synthesized LPG and outer membrane-specific LPG have been published previously (18).

Transcriptional analyses of *mprF* and *dltA*. The transcription of the two genes most frequently linked to DAP^r, *mprF* and *dlt*, was assessed (7, 11, 36, 37). These genes encode proteins involved in lysinylation of membrane phospholipids and alanylation of CW teichoic acids, respectively, each of which can result in a change in the net cell surface charge in *S. aureus* (5, 20, 27, 31, 37). For RNA isolation, fresh overnight cultures of *S. aureus* strains were used to inoculate TSB to an OD_{600} of 0.1. Cells were harvested during both exponential and stationary growth phases. Total RNA was isolated from the cell pellets by using an RNeasy kit (Qiagen, Valencia, CA) and a Fastprep FP120 instrument (Bio 101, Vista, CA), according to the manufacturers' recommended protocols.

Reverse transcriptase (RT)-PCR was performed as described previously (35). The *mprF* cDNA products were detected using primer pair mprF-F and mprF-R (37). The *dlt* cDNA products were detected using primer pair dlt-F and dlt-R (36).

TEM. To determine the CW thicknesses of the strains, cells were prepared for TEM analyses as described previously (3). For each strain, 100 cell wall thickness measurements were taken from a minimum of 50 cells at ×190,000 magnification (model 100CX; Jeol, Tokyo, Japan), as described previously (16). In addition to the seven strain sets outlined above, we employed MRSA strain MU50, a well-characterized prototypical VISA strain (10) known to have thickened CWs. All CW measurements were performed by one of us (C.C.N.) blinded to the iden-

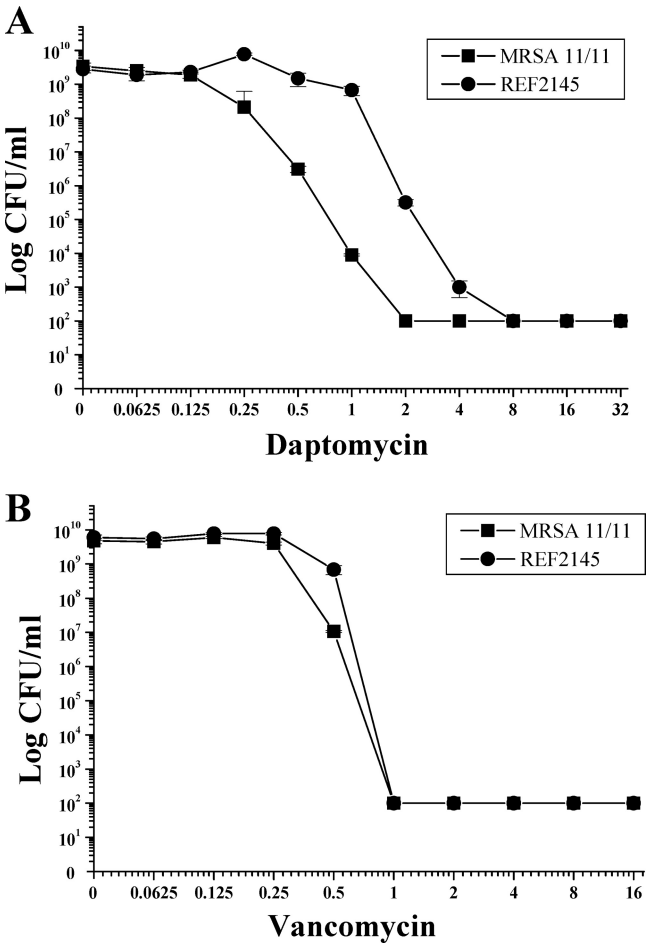

FIG. 1. Population analyses of MRSA 11/11 and REF2145 strains upon exposure to a range of DAP (A) and VAN (B) concentrations. These data represent the means (±SDs) for two separate assays.

tities of the organisms. Differences for which P values were <0.05 were considered statistically significant.

Statistics. Data were analyzed by the Kruskal-Wallis analysis of variance (ANOVA) test, and P values of <0.05 were considered significant.

RESULTS

Population analyses. In population analyses upon exposure to a range of DAP concentrations, the population curve for DAP^r strain REF2145 was shifted substantially to the right, with heterogeneous subpopulations surviving exposures of between 0.125 and 4 μg/ml DAP (Fig. 1A). The AUC values for the population analyses with DAP were 8.41 ± 0.64 and 30.64 ± 1.82 for strains MRSA 11/11 and REF2145, respectively. Population analyses upon exposure of MRSA 11/11 and REF2145 to a range of VAN concentrations revealed survival curves and AUCs very similar to those for DAP (Fig. 1B; AUCs, 5.96 ± 0.03 and 6.65 ± 0.14, respectively).

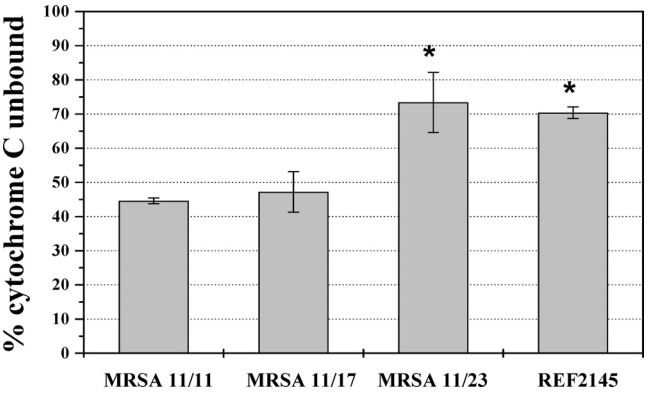

FIG. 2. Binding of positively charged cytochrome *c* to whole *S. aureus* cells. The graph shows the percentage of cytochrome *c* unbound after 10 min of incubation with *S. aureus* at room temperature. Data represent the means and standard deviations from three independent experiments. *, $P < 0.01$ versus MRSA 11/11.

CAP susceptibility. As shown in Table 2, the parental strain, MRSA 11/11, was highly susceptible to tPMP-1 and RP-1, while strain REF2145 was ~6-fold and ~3-fold more resistant to exposures to these peptides, respectively. In contrast, these strains were equally susceptible to the bactericidal activity of hNP-1 (20 μg/ml).

Cell surface charge and binding assays. As shown in Fig. 2, the levels of binding of the positively charged molecule cytochrome *c* to DAP^r MRSA strains 11/21 and REF2145 were significantly less than those to parental strain MRSA 11/11 or the MRSA 11/17 strain ($P < 0.01$). Paralleling the cytochrome *c* binding data, the levels of binding of both DAP and RP-1 were reduced in DAP^r strain REF2145 (Table 2; $P < 0.01$). In agreement with our previous findings (11, 36, 37), these data suggest that the increased repulsion of DAP and CAPs may be due to an increased net positive surface charge in REF2145. Consistent with the VAN MIC and population analysis data, there was no difference in the levels of VAN binding to the DAP^s strains versus those to the DAP^r strains.

Membrane PL profiles. Since the relative proportions of the three major, differentially charged membrane PLs of *S. aureus* can impact the net surface charge, analysis of the PLs was carried out and the results are shown in Table 3. The proportions of the negatively charged PL CL (net charge, −2) were similar among the strains. In contrast to CL, the proportions of PG (net charge, −1) were ~10 and 20% lower in DAP^r strains

TABLE 2. *In vitro* CAP susceptibilities and peptide binding of the primary strain set

Strain	% survival (mean ± SD) after 2h exposure to:			Amt of drug bound (μg/ml)		
	tPMP-1[a] (1 μg/ml)	hNP-1[b] (20 μg/ml)	RP-1[a] (3 μg/ml)	RP-1[a] (40 μg)	DAP[a] (6 μg)	VAN[b] (8 μg)
MRSA 11/11	4 ± 2.0	11 ± 10	6.67 ± 0.57	10.6 ± 3.3	2.03 ± 0.53	1.81 ± 0.13
REF2145	27 ± 10.0	14 ± 11	19.33 ± 2.88	2.82 ± 2.5	0.79 ± 0.45	1.78 ± 0.04

[a] $P < 0.01$.
[b] The results were not significantly different.

TABLE 3. Phospholipid composition and outer membrane translocation of LPG for the primary strain set

Strain	% of total phospholipid content (mean ± SD)				
	Inner LPG	Outer LPG	Total LPG	PG	CL
MRSA 11/11	17.17 ± 1.17	1.73 ± 0.24	18.91 ± 1.41	75.24 ± 1.31	5.86 ± 2.71
MRSA 11/17	18.16 ± 0.38	1.46 ± 0.43	19.63 ± 0.81	72.57 ± 3.89	7.81 ± 3.07
MRSA 11/21	32.15 ± 9.08[a]	2.72 ± 0.54	34.16 ± 8.95[a]	62.45 ± 7.93	5.68 ± 0.61
REF2145	34.67 ± 4.51[a]	2.29 ± 0.49	36.66 ± 4.95[a]	55.25 ± 1.23	7.80 ± 6.23

[a] $P < 0.01$ versus MRSA 11/11 or MRSA 11/17.

11/21 and REF2145, respectively. Of note, the total amounts of positively charged LPG (net charge, +1) were ~2-fold higher in the DAP^r strains than in the DAP^s strains, indicating enhanced synthase function. Importantly, the amount of LPG that was translocated to the outer membrane leaflet was ~6 to 9% of total LPG in all four strains, suggesting similar levels of MprF translocase (flippase) activity among the strains. The net increases in the total amounts of LPG synthesized and ultimately translocated to the outer membrane are consistent with the relative increases in the overall positive surface charge in the DAP^r strains.

Transcriptional analyses of *mprF* and *dlt* genes. As shown in Fig. 3, RT-PCR analysis revealed that the *dlt* transcripts were detected to an equivalent extent, with expression occurring only during exponential growth among all four isolates in the primary strain set. In contrast, the level of transcription of the *mprF* gene was notably increased in the two DAP^r strains compared with that in the two DAP^s strains during exponential growth. This finding correlated well with the phenotype of increased LPG synthesis observed in these DAP^r (see above) strains compared with the phenotype observed in the respective DAP^s isolates.

TEM analyses. As shown in Fig. 4, DAP^r strain 703 (11) had significantly thicker CWs (27.2 ± 3.8 nm) than its DAP^s parental strain, strain 616 (21.9 ± 3.9 nm; $P < 0.05$). Similarly, DAP^r strain BOY 300 exhibited thicker CWs than its DAP^s parental strain, strain BOY 755 (24.9 ± 3.1 versus 28.8 ± 4.1 nm; $P < 0.05$). Importantly, unlike the clinical DAP^r strain sets, strains MRSA 11/21 and REF2145 did not exhibit increased CW thickness measurements compared to those of DAP^s strains ($P > 0.10$) MRSA11/11 and MRSA 11/17 from the same strain set. In examining four other recent DAP^s/DAP^r pairs of clinical strain, there were no significant increases ($P < 0.05$) in CW thickness relative to that of the respective DAP^s strain in three of the four DAP^r strains compared (Table 1). The CWs of one DAP^r strain were significantly thicker than the CWs of the DAP^s parental strain. Thus, among the seven pairs of clinical strains studied, less than 50% (three of seven) of the DAP^r strains exhibited significantly thicker CWs than the respective DAP^s parental strain. The CWs of the one DAP^r strain selected by *in vitro* passage in DAP were significantly thicker than the CWs of the DAP^s parental strain (31.3 ± 2.7 nm and 20.4 ± 2.7 nm, respectively ($P < 0.05$) (16).

Of note, there was no obvious relationship between the levels of the DAP MICs in the DAP^r strains and either the absolute CW thickness measurements or the relative CW thickness differences when the results for individual DAP^r strains and their respective DAP^s parental strains were compared.

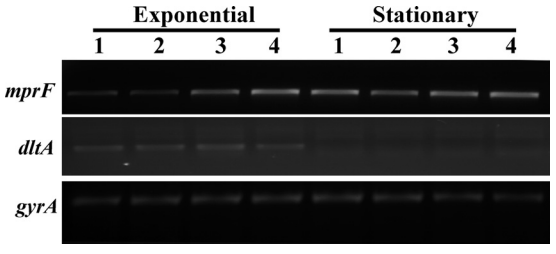

FIG. 3. RT-PCR analyses of *mprF* and *dlt* expression in MRSA 11/11, MRSA 11/17, MRSA 11/23, and REF2145 (lanes 1 to 4, respectively). RNA samples were isolated from exponential- and stationary-phase cultures of the strains and were subjected to RT-PCR to detect transcription of *mprF*, *dltA*, and *gyrA*. The corresponding gels are labeled *mprF*, *dltA*, and *gyrA*, respectively.

DISCUSSION

DAP initiates its bactericidal activity by targeting bacterial CMs, causing rapid CM depolarization and potassium leakage, resulting in DNA, RNA, and protein synthesis inhibition and eventual cell death (24, 25, 29, 30). There have been a number of recent reports of studies with both MSSA and MRSA isolates of the *in vivo* development of DAP^r phenotypes in association with clinical failures (9, 12, 14, 19, 22, 26). However, it

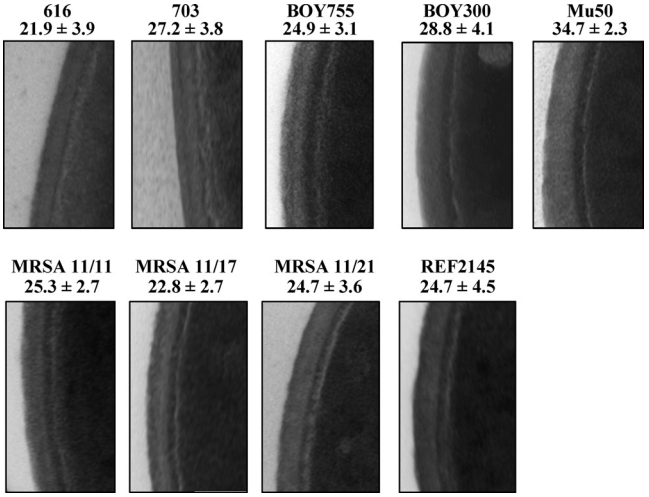

FIG. 4. TEM analyses of the DAP^s and DAP^r *S. aureus* strain sets. The thicknesses of the cell walls were measured at ×190,000 magnification.

appears that there are multiple different mechanism(s) of DAP^r in *S. aureus*, including (i) an enhanced surface positive charge, which results in a charge-repulsive milieu causing reduced DAP binding (11, 36), and (ii) altered membrane fluidity, which perhaps impedes DAP-CM interactions (11, 16).

To expand our knowledge base related to the pathways involved in acquisition of DAP^r phenotypes during DAP treatment failures, we investigated a recent DAP^s/DAP^r strain pair for a range of phenotypic CM and cell surface perturbations, as well as by focused genetic profiling. Several interesting observations emerged from this analysis. There were some similarities in phenotypic assay outcomes between the current strain set and our prior strain set, including enhancement of the cell surface positive charge, a reduction in the level of surface binding by cationic antibiotics and innate host defense CAPs, and the relative resistance to selected CAPs concomitantly with DAP^r (11, 36). One notable difference between the phenotypic characteristics of the strain set from the current study and those described previously was seen in terms of LPG synthesis and the outer membrane translocation of LPG. In prior studies, *mprF* point mutations were associated with the synthesis of equivalent proportional amounts of total LPG between DAP^s and DAP^r isogenic pairs but enhanced outer membrane flipping of LPG (7, 11). In contrast, the current data demonstrate that our DAP^r isolates synthesized increased total amounts of LPG compared with the amounts synthesized by the DAP^s parental strain. However, on a proportional basis, the percentages of the total synthesized LPG which was then translocated to the outer CM leaflet were similar for the DAP^s and DAP^r isolates, suggesting no gain in flipping function among the DAP^r isolates (MRSA 11/21 and REF2145). This enhanced synthesis of LPG in the DAP^r strains, with the overall translocation percentage being maintained at a level equivalent to that in the DAP^s parental isolate, would be expected to yield a net increase in the total number of LPG molecules translocated to the outer membrane leaflet. This notion is in line with the increased cell surface positive charge, as well as the increased CAP- and DAP^r-repulsive phenotypes documented above for the current DAP^r isolates.

One consistent feature of the DAP^r phenotype in VISA strains has been their frequent development of increased CW thickness (4, 6, 16). It has not been determined whether such increased CW thickness in DAP^r strains simply acts as a mechanical barrier to the penetration of this agent so that it may reach its CM target or as a more specific affinity-trapping mechanism for DAP, as suggested for VAN in VISA strains (6). In addition, at this juncture it is not clear whether the biochemical or the genetic pathway is involved in producing such thick CWs in DAP^r strains. To investigate the correlation between CW thickness and DAP^r, TEM analyses were performed on three previously published isogenic sets of *S. aureus* isolates from the bloodstreams of DAP-treated patients in which serial strains exhibited increasing DAP^r in the face of clinical treatment failures (11, 36). Similar to the previous studies of *in vitro*-selected DAP^r (4, 6, 16), strains DAP^r 703 and BOY 300 demonstrated significantly thicker CWs than their DAP^s parental strains, strains 616 and BOY 755, respectively. However, in contrast to the findings for these strain sets, the currently studied strains, DAP^r strains MRSA 11/21 and REF2145, showed no difference in CW thickness from that of their parental MRSA 11/11 strain. These findings suggest that the development of DAP^r in this strain set does not require significant CW perturbations. Substantiating this interpretation, phenotypic readouts of CW function assessed from the Triton X-100-induced autolysis profiles of DAP^s strains MRSA 11/11 and MRSA 11/17 were virtually identical to those of DAP^r strains MRSA 11/21 and REF2145 (data not shown). Thus, these data support the notion that CW abnormalities do not underlie the DAP^r phenotype in the present strain set. Furthermore, three of four additional recent clinical DAP^s/DAP^r strain pairs showed no evidence of thickened CWs among the DAP^r isolates. Transcriptomic and proteomic comparisons of DAP^s/DAP^r strain pairs are in progress to clarify whether specific metabolic pathways have a potential role in the thick CW phenotype.

Lastly, our laboratory has shown that the profiles of the enhanced expression of the *mprF* and/or *dlt* gene are intimately related to the maintenance of a relatively high positive surface charge in DAP^r (compared with that in DAP^s) *S. aureus* strains (11, 36, 37). Unlike previously characterized DAP^r strain BOY 300 (36), RT-PCR analysis revealed comparable levels of *dlt* expression between DAP^s (MRSA 11/11 and MRSA 11/17)

TABLE 4. Correlates of DAP^r among recent S. aureus isolates: comparison with current DAP^s and DAP^r primary strain set

DAP^r strain(s)	Source	Increased positive surface charge	Potential mechanism(s) of increased positive surface	Genetic factor(s) potentially involved in surface charge alterations	CW thickness	Reference
CB2205 (MRSA MW2 USA 400)	*In vitro* selection by serial passage in DAP	No	NA[a]	NA	↑[b]	16
701, 703 (MSSA[c])	Clinical isolates - endocarditis	Yes	Increased LPG translocation to outer membrane leaflet	Increased *mprF* transcription (stationary phase), S295L point mutation	↑	11, 37
BOY300 (MSSA)	Clinical isolate - endocarditis	Yes	Increased teichoic acid alanylation	Increased *dlt* transcription	↑	36
MRSA 11/21, REF2145 (MRSA USA 300)	Clinical isolates - endocarditis	Yes	Increased total LPG synthesis	Increased *mprF* transcription (exponential phase), T345A point mutation	Equivalent	This study

[a] NA, not applicable.
[b] ↑, increased.
[c] MSSA, methicillin-susceptible *S. aureus*.

and DAP^r (MRSA 11/21 and REF2145) strains. In contrast to *dlt* expression, the two DAP^r strains evaluated in the current study exhibited increased levels of *mprF* transcription compared with those of the respective DAP^s strains during exponential growth, correlating proportionally with increased levels of synthesis of LPG in these strains. This *mprF* overexpression profile of MRSA 11/21 and REF2145 differs from that of previously characterized DAP^r strains 701 and 703. In these DAP^r strains, *mprF* overexpression occurred during stationary growth phase, was associated with a point mutation in the putative translocase domain of the *mprF* gene product (Ser to Leu at position 295), and was phenotypically associated with enhanced LPG flipping to the outer membrane leaflet of the DAP^r isolate (11, 37). Interestingly, the point mutation noted within the *mprF* gene of MRSA 11/21 and REF2145 resides in the putative synthase domain of the MprF protein (Thr to Ala at position 345) (7, 19), consistent with enhanced LPG synthesis relative to that in the DAP^s parental strains. Therefore, these data reinforce our previous hypothesis that DAP resistance is associated with *mprF* mutations that result in a gain of function for either LPG synthesis and/or translocation (11, 37). Whether *mprF* point mutations can fully account for DAP^r is the topic of current studies in our laboratory, utilizing mutated *mprF* genes from DAP^r strains cloned into DAP^s background strains.

We have summarized the current and previous studies from our laboratory in Table 4 (11, 16, 36, 37). The information in Table 4 relates CW thickness, *dlt* and *mprF* mutations, gains in *mprF* function in PL synthesis/translocation, as well as surface charge and peptide binding perturbations. These comparative data underscore the concept that DAP^r is a final common pathway that may be arrived at by multiple and distinct mechanisms.

In summary, although a common accompaniment of DAP^r in *S. aureus*, CW thickening is not a universal finding. This suggests that additional pathways and mechanisms leading to the DAP^r phenotype manifested by the current strain set are in play. We speculate that the best explanation for the DAP^r phenotype in the latter strain set involves the excess proportional synthesis of LPG with an ultimately increased net outer leaflet localization of this cationic PL, yielding reduced DAP access to or an association with vulnerable targets on the organism's surface.

ACKNOWLEDGMENTS

This research was supported by grants from the National Institutes of Health to A.S.B. (grant AI39018) and M.R.Y. (grant AI39001).

REFERENCES

1. **Bharat, L. D., and M. G. Chhitar.** 1998. Role of the actin cytoskeleton in regulating the outer phosphatidylethanolamine levels in yeast plasma membrane. Eur. J. Biochem. **254:**202–206.
2. **Boucher, H. W., and G. Sakoulas.** 2007. Antimicrobial resistance: perspectives on daptomycin resistance, with emphasis on resistance in *Staphylococcus aureus*. Clin. Infect. Dis. **45:**601–608.
3. **Brunskill, E. W., and K. W. Bayles.** 1996. Identification and molecular characterization of a putative regulatory locus that affects autolysis in *Staphylococcus aureus*. J. Bacteriol. **178:**611–618.
4. **Camargo, I. L, H.-M. Neoh, L. Cui, and K. Hiramatsu.** 2008. Serial daptomycin selection generates daptomycin-nonsusceptible *Staphylococcus aureus* strains with a heterogeneous vancomycin-intermediate phenotype. Antimicrob. Agents Chemother. **52:**4289–4299.
5. **Collins, L. V., S. A. Kristian, C. Weidenmaier, M. Faigle, K. P. M. van Kessel, J. A. G. van Strijp, F. Gotz, B. Neumeister, and A. Peschel.** 2002. *Staphylococcus aureus* strains lacking d-alanine modifications of teichoic acids are highly susceptible to human neutrophil killing and are virulence attenuated in mice. J. Infect. Dis. **186:**214–219.
6. **Cui, L., E. Tominaga, H.-M. Neoh, and K. Hiramatsu.** 2006. Correlation between reduced daptomycin susceptibility and vancomycin resistance in vancomycin-intermediate *Staphylococcus aureus*. Antimicrob. Agents Chemother. **50:**1079–1082.
7. **Ernst, C., P. Staubitz, N. N. Mishra, S. J. Yang, G. Hornig, H. Kalbacher, A. S. Bayer, D. Kraus, and A. Peschel.** 2009. The bacterial defensin resistance protein MprF consists of separable domains for lipid lysinylation and antimicrobial peptide repulsion. PLos Pathog. **5:**e1000660.
8. **Friedman, L., J. D. Alder, and J. A. Silverman.** 2006. Genetic changes that correlate with reduced susceptibility to daptomycin in *Staphylococcus aureus*. Antimicrob. Agents Chemother. **50:**2137–2145.
9. **Hayden, M. K., K. Rezai, R. A. Hayes, K. Lolans, J. P. Quinn, and R. A. Weinstein.** 2005. Development of daptomycin resistance *in vivo* in methicillin-resistant *Staphylococcus aureus*. J. Clin. Microbiol. **43:**5285–5287.
10. **Hiramatsu, K., H. Hanaki, T. Ino, K. Yabuta, T. Oguri, and F. C. Tenover.** 1997. Methicillin-resistant *Staphylococcus aureus* clinical strain with reduced vancomycin susceptibility. J. Antimicrob. Chemother. **40:**135–136.
11. **Jones, T., M. R. Yeaman, G. Sakoulas, S. J. Yang, R. A. Proctor, H. G. Sahl, J. Schrenzel, Y. Q. Xiong, and A. S. Bayer.** 2008. Failures in clinical treatment of *Staphylococcus aureus* infection with daptomycin are associated with alterations in surface charge, membrane phospholipid asymmetry, and drug binding. Antimicrob. Agents Chemother. **52:**269–278.
12. **Julian, K., K. Kosowska-Shick, C. Whitener, M. Roos, H. Labischinski, A. Rubio, L. Parent, L. Ednie, L. Koeth, T. Bogdanovich, and P. C. Appelbaum.** 2007. Characterization of a daptomycin-nonsusceptible vancomycin-intermediate *Staphylococcus aureus* strain in a patient with endocarditis. Antimicrob. Agents Chemother. **51:**3445–3448.
13. **Lalani, T., J. J. Federspiel, H. W. Boucher, T. H. Rude, I.-G. Bae, M. J. Rybak, G. T. Tonthat, G. R. Corey, M. E. Stryjewski, G. Sakoulas, V. H. Chu, J. Alder, J. N. Steenbergen, S. A. Luperchio, M. Campion, C. W. Woods, and V. G. Fowler.** 2008. Associations between the genotypes of *Staphylococcus aureus* bloodstream isolates and clinical characteristics and outcomes of bacteremic patients. J. Clin. Microbiol. **46:**2890–2896.
14. **Mariani, P. G., H. S. Sader, and R. N. Jones.** 2006. Development of decreased susceptibility to daptomycin and vancomycin in a *Staphylococcus aureus* strain during prolonged therapy. J. Antimicrob. Chemother. **58:**481–483.
15. **Meehl, M., S. Herbert, F. Gotz, and A. Cheung.** 2007. Interaction of the GraRS two-component system with the VraFG ABC transporter to support vancomycin-intermediate resistance in *Staphylococcus aureus*. Antimicrob. Agents Chemother. **51:**2679–2689.
16. **Mishra, N. N., S. J. Yang, A. Sawa, A. Rubio, C. C. Nast, M. R. Yeaman, and A. S. Bayer.** 2009. Analysis of cell membrane characteristics of *in vitro*-selected daptomycin-resistant strains of methicillin-resistant *Staphylococcus aureus* (MRSA). Antimicrob. Agents Chemother. **53:**2312–2318.
17. **Moore, M. R., F. Perdreau-Remington, and H. F. Chambers.** 2003. Vancomycin treatment failure associated with heterogeneous vancomycin-intermediate *Staphylococcus aureus* in a patient with endocarditis and in the rabbit model of endocarditis. Antimicrob. Agents Chemother. **47:**1262–1266.
18. **Mukhopadhyay, K., W. Whitmire, Y. Q. Xiong, J. Molden, T. Jones, A. Peschel, P. Staubitz, J. Adler-Moore, P. J. McNamara, R. A. Proctor, M. R. Yeaman, and A. S. Bayer.** 2007. *In vitro* susceptibility of *Staphylococcus aureus* to thrombin-induced platelet microbicidal protein-1 (tPMP-1) is influenced by cell membrane phospholipid composition and asymmetry. Microbiology **153:**1187–1197.
19. **Murthy, M. H., M. E. Olson, R. E. Wickert, P. D. Fey, and Z. Jalali.** 2008. Daptomycin non-susceptible methicillin-resistant *Staphylococcus aureus* USA 300 isolate. J. Med. Microbiol. **57:**1036–1038.
20. **Oku, Y., K. Kurokawa, N. Ichihashi, and K. Sekimizu.** 2004. Characterization of the *Staphylococcus aureus mprF* gene, involved in lysinylation of phosphatidylglycerol. Microbiology **150:**45–51.
21. **Peschel, A., M. Otto, R. W. Jack, H. Kalbacher, G. Jung, and F. Gotz.** 1999. Inactivation of the *dlt* operon in *Staphylococcus aureus* confers sensitivity to defensins, protegrins, and other antimicrobial peptides. J. Biol. Chem. **274:**8405–8410.
22. **Pillai, S. K., H. S. Gold, G. Sakoulas, C. Wennersten, R. C. Moellering, Jr., and G. M. Eliopoulos.** 2007. Daptomycin nonsusceptibility in *Staphylococcus aureus* with reduced vancomycin susceptibility is independent of alterations in MprF. Antimicrob. Agents Chemother. **51:**2223–2225.
23. **Sakoulas, G., G. M. Eliopoulos, J. Alder, and C. T. Eliopoulos.** 2003. Efficacy of daptomycin in experimental endocarditis due to methicillin-resistant *Staphylococcus aureus*. Antimicrob. Agents Chemother. **47:**1714–1718.
24. **Schriever, C. A., C. Fernandez, K. A. Rodvold, and L. H. Danziger.** 2005. Daptomycin: a novel cyclic lipopeptide antimicrobial. Am. J. Health Syst. Pharm. **62:**1145–1158.
25. **Silverman, J. A., N. G. Perlmutter, and H. M. Shapiro.** 2003. Correlation of daptomycin bactericidal activity and membrane depolarization in *Staphylococcus aureus*. Antimicrob. Agents Chemother. **47:**2538–2544.

26. **Skiest, D. J.** 2006. Treatment failure resulting from resistance of *Staphylococcus aureus* to daptomycin. J. Clin. Microbiol. **44:**655–656.
27. **Staubitz, P., H. Neumann, T. Schneider, I. Wiedemann, and A. Peschel.** 2004. MprF-mediated biosynthesis of lysylphosphatidylglycerol, an important determinant in staphylococcal defensin resistance. FEMS Microbiol. Lett. **231:**67.
28. **Steenbergen, J. N., J. Alder, G. M. Thorne, and F. P. Tally.** 2005. Daptomycin: a lipopeptide antibiotic for the treatment of serious Gram-positive infections. J. Antimicrob. Chemother. **55:**283–288.
29. **Straus, S. K., and R. E. W. Hancock.** 2006. Mode of action of the new antibiotic for Gram-positive pathogens daptomycin: comparison with cationic antimicrobial peptides and lipopeptides. Biochim. Biophys. Acta **1758:** 1215.
30. **Tally, F. P., and M. F. DeBruin.** 2000. Development of daptomycin for Gram-positive infections. J. Antimicrob. Chemother. **46:**523–526.
31. **Weidenmaier, C., A. Peschel, V. A. J. Kempf, N. Lucindo, M. R. Yeaman, and A. S. Bayer.** 2005. DltABCD- and MprF-mediated cell envelope modifications of *Staphylococcus aureus* confer resistance to platelet microbicidal proteins and contribute to virulence in a rabbit endocarditis model. Infect. Immun. **73:**8033–8038.
32. **Wootton, M., A. P. MacGowan, and T. R. Walsh.** 2006. Comparative bactericidal activities of daptomycin and vancomycin against glycopeptide-intermediate *Staphylococcus aureus* (GISA) and heterogeneous GISA isolates. Antimicrob. Agents Chemother. **50:**4195–4197.
33. **Xiong, Y. Q., A. S. Bayer, L. Elazegui, and M. R. Yeaman.** 2006. A synthetic congener modeled on a microbicidal domain of thrombin-induced platelet microbicidal protein-1 recapitulates staphylocidal mechanisms of the native molecule. Antimicrob. Agents Chemother. **50:**3786–3792.
34. **Xiong, Y. Q., K. Mukhopadhyay, M. R. Yeaman, J. Adler-Moore, and A. S. Bayer.** 2005. Functional interrelationships between cell membrane and cell wall in antimicrobial peptide-mediated killing of *Staphylococcus aureus*. Antimicrob. Agents Chemother. **49:**3114–3121.
35. **Yang, S.-J., K. C. Rice, R. J. Brown, T. G. Patton, L. E. Liou, Y. H. Park, and K. W. Bayles.** 2005. A LysR-type regulator, CidR, is required for induction of the *Staphylococcus aureus cidABC* operon. J. Bacteriol. **187:**5893–5900.
36. **Yang, S. J., B. N. Kreiswirth, G. Sakoulas, M. R. Yeaman, Y. Q. Xiong, A. Sawa, and A. S. Bayer.** 2009. Enhanced expression of *dltABCD* is associated with development of daptomycin nonsusceptibility in a clinical endocarditis isolate of *Staphylococcus aureus*. J. Infect. Dis. **200:**1916–1920.
37. **Yang, S. J., Y. Q. Xiong, P. M. Dunman, J. Schrenzel, P. Francois, A. Peschel, and A. S. Bayer.** 2009. Regulation of *mprF* in daptomycin-nonsusceptible *Staphylococcus aureus*. Antimicrob. Agents Chemother. **53:**2636–2637.
38. **Yeaman, M. R., A. S. Bayer, S.-P. Koo, W. Foss, and P. M. Sullam.** 1998. Platelet microbicidal proteins and neutrophil defensin disrupt the *Staphylococcus aureus* cytoplasmic membrane by distinct mechanisms of action. J. Clin. Invest. **101:**178–187.
39. **Yeaman, M. R., K. D. Gank, A. S. Bayer, and E. P. Brass.** 2002. Synthetic peptides that exert antimicrobial activities in whole blood and blood-derived matrices. Antimicrob. Agents Chemother. **46:**3883–3891.
40. **Yeaman, M. R., S. M. Puentes, D. C. Norman, and A. S. Bayer.** 1992. Partial characterization and staphylocidal activity of thrombin-induced platelet microbicidal protein. Infect. Immun. **60:**1202–1209.